ISSN: 2689-1204

Research Article

Journal of Applied Material Science & Engineering Research

Based on Natural Intelligence and Artificial Intelligence Techniques to Determine both Carbohydrates and Sugar Intake Amount and PPG Predictions Using Viscoplastic Energy Model of GH-Method: Math-Physical Medicine (No. 1030, Viscoelastic Medicine Theory #428)

Gerald C. Hsu

EclaireMD Foundation, USA

*Corresponding Author
Gerald C. Hsu, EclaireMD Foundation, USA

Submitted: 2024, Feb 26; **Accepted:** 2024, Mar 18; **Published:** 2024, Mar 28

Citation: Hsu, G. C. (2024). Based on Natural Intelligence and Artificial Intelligence Techniques to Determine both Carbohydrates and Sugar Intake Amount and PPG Predictions Using Viscoplastic Energy Model of GH-Method: Math-Physical Medicine (No. 1030, Viscoelastic Medicine Theory #428). *J App Mat Sci & Engg Res, 8*(1), 01-07.

Category: Methodology & Diabetes

Abstract

The molecular structures of plants and animals display a variety of colors with different color shades, each corresponding to a unique optical wave with distinct frequency, amplitude, and wavelength. To capture these nuances, the author employs a 12-megapixel camera on his Apple iPhone 13, allowing for high-resolution imaging. This rich dataset enables precise differentiation of color shades, thanks to the iPhone's computational power and user convenience.

Utilizing this capability, the author has developed a unique mathematical algorithm that maps these 12-megapixel color data to the three fundamental properties of color waves of food and meals, facilitating the analysis of consumed food's internal makeup, such as carbohydrate and sugar content—vital information for managing his diabetes. This system, dubbed "Carbs AI" (artificial intelligence), is enhanced by the author's self-learned extensive knowledge of food nutrition, acquired over past 15 years and referred to as "Carbs NI" (natural intelligence). The method calculates postprandial plasma glucose (PPG) levels by combining linear elasticity theory with fasting plasma glucose (FPG) and post-meal step count (Steps), two other significant factors affecting PPG.

Drawing on his personal data collected within past 10 years from May 1, 2015, to February 5, 2024, the author explores PPG prediction via AI and NI, integrating three inputs from both Carbs AI and NI, FPG, and Steps. This study also evaluates the prediction accuracy and curve correlation between AI and NI models with their vital energy distributions information using the space-domain viscoplastic theory and energy model (SD-VMT).

***In summary,** the findings reveal that the Carbs AI and Carbs NI models achieve 95% prediction accuracy and 68% correlation. Additionally, the PPG AI and PPG NI models attain 99% prediction accuracy and 99% of correlation.*
The SD-VMT approach outlines energy distributions for PPG and Carbs, highlighting identical outcomes except in time-zone energy distributions.
Insulin (FPG): 40%,
Carbs (energy intake): 36%,
Steps (energy expenditure): 24%.
*It is specifically noted that **Carbs to Steps ratio is around 1.5** which means **diet is more important than exercise**.*
Time-zone energy distributions between AI and NI are different for Carbs and PPG, as follows:
For Carbs:
62% for Y15-Y19 vs. 38% for Y29-Y24.
For PPG:
54% for Y15-Y19 vs. 46% for Y29-Y24.

Key Message

The author demonstrates that AI technology, grounded in optical physics and wave theory, delivers high predictive accuracy and valuable insights into the interplay between beta cell insulin status, physical activity, and carbohydrate/sugar intake amount.

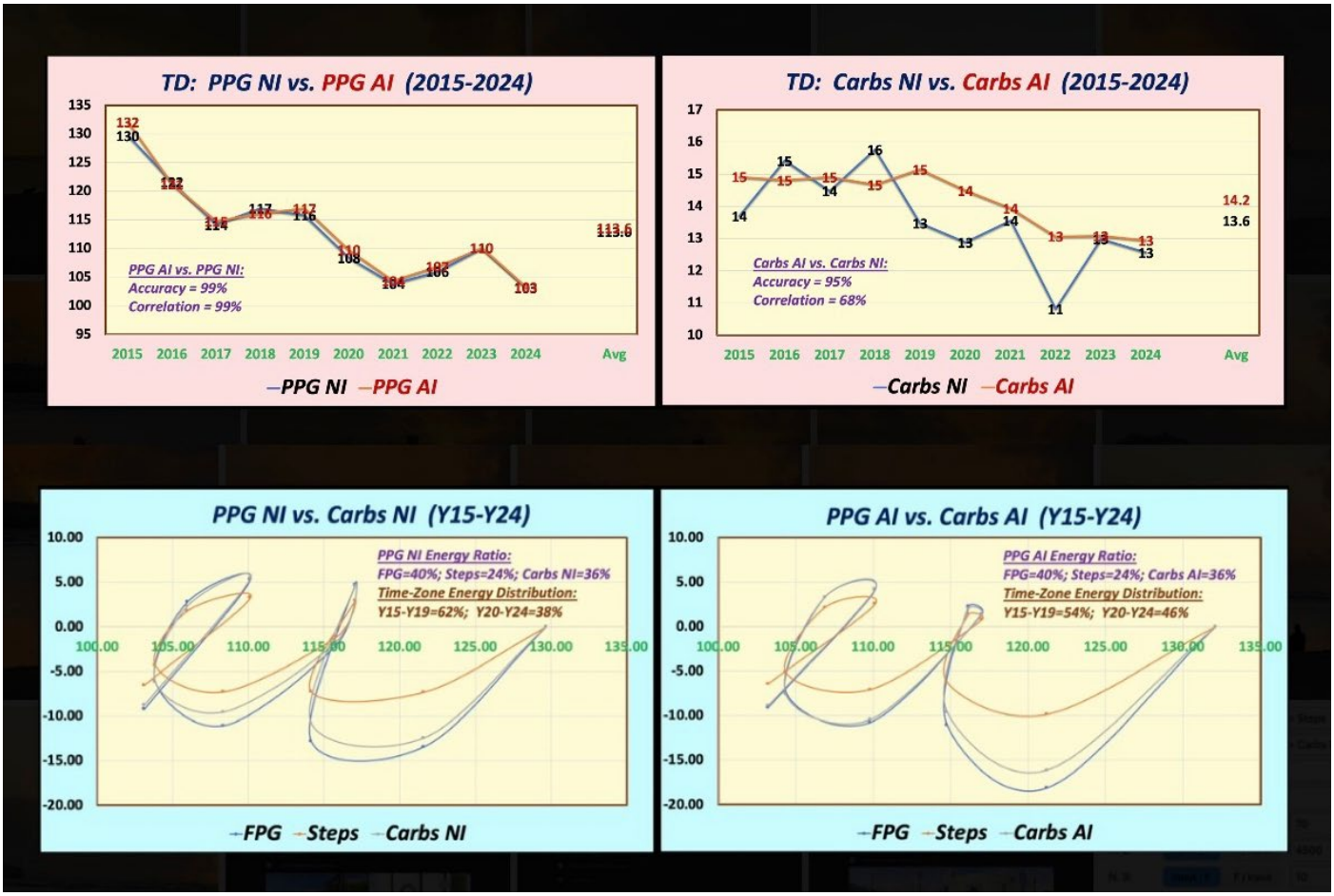

1. Introduction

The molecular structures of plants and animals display a variety of colors with different color shades, each corresponding to a unique optical wave with distinct frequency, amplitude, and wavelength. To capture these nuances, the author employs a 12-megapixel camera on his Apple iPhone 13, allowing for high-resolution imaging. This rich dataset enables precise differentiation of color shades, thanks to the iPhone's computational power and user convenience.

Utilizing this capability, the author has developed a unique mathematical algorithm that maps these 12-megapixel color data to the three fundamental properties of color waves of food and meals, facilitating the analysis of consumed food's internal makeup, such as carbohydrate and sugar content—vital information for managing his diabetes. This system, dubbed "Carbs AI" (artificial intelligence), is enhanced by the author's self-learned extensive knowledge of food nutrition, acquired over past 15 years and referred to as "Carbs NI" (natural intelligence). The method calculates postprandial plasma glucose (PPG) levels by combining linear elasticity theory with fasting plasma glucose (FPG) and post-meal step count (Steps), two other significant factors affecting PPG.

Drawing on his personal data collected within past 10 years from May 1, 2015, to February 5, 2024, the author explores PPG prediction via AI and NI, integrating three inputs from both Carbs AI and NI, FPG, and Steps. This study also evaluates the prediction accuracy and curve correlation between AI and NI models with their vital energy distributions information using the space-domain viscoplastic theory and energy model (SD-VMT).

1.1 Biomedical and Engineering or Technical information

The following sections contain excerpts and concise information on meticulously reviewed by the author of this paper. The author has adopted this approach as an alternative to including a conventional reference list at the end of this document, with the intention of optimizing his valuable research time. It is essential to clarify that these sections do not constitute part of the author's original contribution but have been included to aid the author in his future reviews and offer valuable insights to other readers with an interest in these subjects.

2. Relationship between Colors of Plant Food or Animal Food versus Exterior Colors?

The relationship between the colors of plant-based and animal-

based foods and their external appearances can vary. In general, the exterior colors of foods derived from plants and animals can offer insights into their nutritional content, ripeness, freshness, and sometimes even their flavor profiles.

2.1 Plants

The exterior colors of fruits, vegetables, and other plant-based foods often provide visual cues about their potential health benefits and nutritional content. For instance, vibrant and varied colors in fruits and vegetables are often associated with higher concentrations of essential nutrients, such as vitamins, minerals, and antioxidants. The color intensity may also indicate ripeness and can influence the taste and appeal of the food.

2.2 Animals

When it comes to animal-based foods, such as meats, the external appearance and color can also convey important information. The color of meat, for example, can indicate its freshness or the presence of specific nutrients. Additionally, the color of eggs and fish can also provide valuable information about their quality and nutrient content.

In both plant-based and animal-based foods, colors can signify freshness, ripeness, nutritional value, and even individual taste preferences. Understanding the relationship between the exterior colors of food and their inherent qualities can aid in making informed decisions about dietary choices and meal planning.

(Note: The author pays his special interest in the nutritional values of both plant-based and animal-based food materials.).

3. The influences on good nutritions and their color changes during food cooking process:

The influence of cooking on the nutritional content and color of foods can vary depending on the cooking method and the type of food being prepared.

3.1 Nutritional Changes

Cooking can lead to both positive and negative changes in the nutritional content of foods. For example, while some cooking methods can enhance the bioavailability of certain nutrients, others may lead to nutrient loss. For instance, boiling vegetables can result in the loss of water-soluble vitamins, such as vitamin C, while steaming or microwaving may preserve more of these nutrients.

3.2 Color Changes

The cooking process often causes changes in the color of food. For instance, heat can cause the Maillard reaction, which leads to the browning of some foods, resulting in new and complex flavor compounds. This reaction can transform the original color of food, such as the browning of meats and baked goods. On the other hand, some vegetables may lose their vibrant colors during cooking due to the breakdown of pigments and exposure to heat and water.

3.3 Impact of Color Changes

While color changes during cooking may affect the aesthetics of food, they can also influence the perception of flavor and the appeal of the dish. For example, the browning of certain foods can enhance the taste and aroma, while the loss of vibrant colors in vegetables may impact their visual appeal.

It's important to consider the impact of cooking on both the nutritional content and color changes of foods to make informed decisions about meal preparation. Understanding how different cooking methods affect the nutritional value and color of foods can help optimize the retention of nutrients and preserve the visual appeal of dishes.
(Note: The author's AI algorithm can automatically distinguish both uncooked and cooked food material.)

4. MPM Background

To learn more about his developed GH-Method: math-physical medicine (MPM) methodology, readers can read the following three papers selected from his published 760+ papers.

The first paper, No. 386 (Reference 1) describes his MPM methodology in a general conceptual format. The second paper, No. 387 (Reference 2) outlines the history of his personalized diabetes research, various application tools, and the differences between biochemical medicine (BCM) approach versus the MPM approach. The third paper, No. 397 (Reference 3) depicts a general flow diagram containing ~10 key MPM research methods and different tools.

5. The Author's Diabetes History

The author was a severe T2D patient since 1995. He weighed 220 lb. (100 kg) at that time. By 2010, he still weighed 198 lb. with an average daily glucose of 250 mg/dL (HbA1C at 10%). During that year, his triglycerides reached 1161 (high risk for CVD and stroke) and his albumin-creatinine ratio (ACR) at 116 (high risk for chronic kidney disease). He also suffered from five cardiac episodes within a decade. In 2010, three independent physicians warned him regarding the need for kidney dialysis treatment and the future high risk of dying from his severe diabetic complications.

In 2010, he decided to self-study endocrinology with an emphasis on diabetes and food nutrition. He spent the entire year of 2014 to develop a metabolism index (MI) mathematical model. During 2015 and 2016, he developed four mathematical prediction models related to diabetes conditions: weight, PPG, fasting plasma glucose (FPG), and HbA1C (A1C). Through using his developed mathematical metabolism index (MI) model and the other four glucose prediction tools, by the end of 2016, his weight was reduced from 220 lbs. (100 kg) to 176 lbs. (89 kg), waistline from 44 inches (112 cm) to 33 inches (84 cm), average finger-piercing glucose from 250 mg/dL to 120 mg/dL, and A1C from 10% to ~6.5%. One of his major accomplishments is that he no longer takes any diabetes-related medications since 12/8/2015.

In 2017, he achieved excellent results on all fronts, especially his glucose control. However, during the pre-COVID period, including both 2018 and 2019, he traveled to ~50 international

cities to attend 65+ medical conferences and made ~120 oral presentations. This hectic schedule inflicted damage to his diabetes control caused by stress, dining out frequently, post-meal exercise disruption, and jet lag, along with the overall negative metabolic impact from the irregular life patterns; therefore, his glucose control was somewhat affected during the two-year traveling period of 2018-2019.

He started his COVID-19 self-quarantined life on 1/19/2020. By 10/16/2022, his weight was further reduced to ~164 lbs. (BMI 24.22) and his A1C was at 6.0% without any medication intervention or insulin injection. In fact, with the special COVID-19 quarantine lifestyle since early 2020, not only has he written and published ~500 new research articles in various medical and engineering journals, but he has also achieved his best health conditions for the past 27 years. These achievements have resulted from his non-traveling, low-stress, and regular daily life routines. Of course, his in-depth knowledge of chronic diseases, sufficient practical lifestyle management experiences, and his own developed high-tech tools have also contributed to his excellent health improvements.

On 5/5/2018, he applied a continuous glucose monitoring (CGM) sensor device on his upper arm and checks his glucose measurements every 5 minutes for a total of 288 times each day. Furthermore, he extracted the 5-minute intervals from every 15-minute interval for a total of 96 glucose data each day stored in his computer software.

Through the author's medical research work over 40,000 hours and read over 4,000 published medical papers online in the past 13 years, he discovered and became convinced that good life habits of not smoking, moderate or no alcohol intake, avoiding illicit drugs; along with eating the right food with well-balanced nutrition, persistent exercise, having a sufficient and good quality of sleep, reducing all kinds of unnecessary stress, maintaining a regular daily life routine contribute to the risk reduction of having many diseases, including CVD, stroke, kidney problems, micro blood vessels issues, peripheral nervous system problems, and even cancers and dementia. In addition, a long-term healthy lifestyle can even "repair" some damaged internal organs, with different required time-length depending on the particular organ's cell lifespan. For example, he has "self-repaired" about 35% of his damaged pancreatic beta cells during the past 10 years.

6. Energy Theory

The human body and organs have around 37 trillion live cells which are composed of different organic cells that require energy infusion from glucose carried by red blood cells; and energy consumption from labor-work or exercise. When the residual energy (resulting from the plastic glucose scenario) is stored inside our bodies, it will cause different degrees of damage or influence to many of our internal organs.

According to physics, energies associated with the glucose waves are proportional to the square of the glucose amplitude. The residual energies from elevated glucoses are circulating inside the body via blood vessels which then impact all of the internal organs to cause different degrees of damage or influence, e.g. diabetic complications. Elevated glucose (hyperglycemia) causes damage to the structural integrity of blood vessels. When it combines with both hypertension (rupture of arteries) and hyperlipidemia (blockage of arteries), CVD or Stroke happens. Similarly, many other deadly diseases could result from these excessive energies which would finally shorten our lifespan. For an example, the combination of hyperglycemia and hypertension would cause micro-blood vessel's leakage in kidney systems which is one of the major cause of CKD.

The author then applied Fast Fourier Transform (FFT) operations to convert the input wave from a time domain into a frequency domain. The y-axis amplitude values in the frequency domain indicate the proportional energy levels associated with each different frequency component of input occurrence. **Both output symptom value (i.e. strain amplitude in the time domain) and output symptom fluctuation rate (i.e. the strain rate and strain frequency) are influencing the energy level (i.e. the Y-amplitude in the frequency domain).**

Currently, many people live a sedentary lifestyle and lack sufficient exercise to burn off the energy influx which causes them to become overweight or obese. Being overweight and having obesity leads to a variety of chronic diseases, particularly diabetes. In addition, many types of processed food add unnecessary ingredients and harmful chemicals that are toxic to the bodies, which lead to the development of many other deadly diseases, such as cancers. For example, ~85% of worldwide diabetes patients are overweight, and ~75% of patients with cardiac illnesses or surgeries have diabetes conditions.

In engineering analysis, when the load is applied to the structure, it bends or twists, i.e. deform; however, when the load is removed, it will either be restored to its original shape (i.e, elastic case) or remain in a deformed shape (i.e. plastic case). In a biomedical system, the glucose level will increase after eating carbohydrates or sugar from food; therefore, the carbohydrates and sugar function as the energy supply. After having labor work or exercise, the glucose level will decrease. As a result, the exercise burns off the energy, which is similar to load removal in the engineering case. In the biomedical case, both processes of energy influx and energy dissipation take some time which is not as simple and quick as the structural load removal in the engineering case. Therefore, the age difference and 3 input behaviors are "dynamic" in nature, i.e. time-dependent. *This time-dependent nature leads to a "viscoelastic or viscoplastic" situation*. **For the author's case, it is "viscoplastic" since most of his biomarkers are continuously improved during the past 13-year time window.**

Time-dependent output strain and stress of (viscous input*output rate)

Hooke's law of linear elasticity is expressed as:

Strain (ε: epsilon)
= Stress (σ: sigma) / Young's modulus (E)

For biomedical glucose application, his developed linear elastic glucose theory (LEGT) is expressed as:

PPG (strain) = carbs/sugar (stress) * GH.p-Modulus (a positive number) + post-meal walking k-steps * GH.w-Modulus (a negative number)

Where GH.p-Modulus is reciprocal of Young's modulus E.

However, in viscoelasticity or viscoplasticity theory, the stress is expressed as:

Stress
= viscosity factor (η: eta) * strain rate (dε/dt)

Where strain is expressed as Greek epsilon or ε.

In this article, in order to construct an "ellipse-like" diagram in a stress-strain space domain (e.g. "hysteresis loop") covering both the positive side and negative side of space, he has modified the definition of strain as follows:

Strain
= (body weight at certain specific time instant)

He also calculates his strain rate using the following formula:

Strain rate
= (body weight at next time instant) - (body weight at present time instant)

The risk probability % of developing into CVD, CKD, Cancer is calculated based on his developed metabolism index model (MI) in 2014. His MI value is calculated using inputs of 4 chronic conditions, i.e. weight, glucose, blood pressure, and lipids; and 6 lifestyle details, i.e. diet, drinking water, exercise, sleep, stress, and daily routines. These 10 metabolism categories further contain ~500 elements with millions of input data collected and processed since 2010. For individual deadly disease risk probability %, his mathematical model contains certain specific weighting factors for simulating certain risk percentages associated with different deadly diseases, such as metabolic disorder-induced CVD, stroke, kidney failure, cancers, dementia; artery damage in heart and brain, micro-vessel damage in kidney, and immunity-related infectious diseases, such as COVID death.

Some of explored deadly diseases and longevity characteristics using the ***viscoplastic medicine theory (VMT)*** include stress relaxation, creep, hysteresis loop, and material stiffness, damping effect ***based on time-dependent stress and strain*** which are different from his previous research findings using ***linear elastic glucose theory (LEGT) and nonlinear plastic glucose theory (NPGT).***

7. Results

NI					/ 70	/ 4500	/10	S. Rate	Strain	Strs 1	Strs 2	Strs 3	Hgt 1	Hgt 2	Hgt 3	Area 1	Area 2	Area 3	Time	Pred.	Pred.	Pred.
2/6/24	PPG NI	FPG	Steps	Carbs NI	FPG	Steps	Carbs NI	PPG NI	PPG NI	FPG	Steps	Carbs NI	FPG	Steps	Carbs NI	FPG	Steps	Carbs NI	Zone	Step 1	Step 2	PPG NI
2015	130	123	3036	13.7	1.76	0.67	1.37	0.00	129.69	0.00	0.00	0.00	0.00	0.00	0.00	0	0	0	Y15-Y19	1.36	1.04	129.69
2016	122	117	4084	15.4	1.67	0.91	1.54	-8.08	121.61	-13.46	-7.33	-12.46	-6.73	-3.67	-6.23	54	30	50	342	1.44	1.1	124.24
2017	114	120	4382	14.5	1.72	0.97	1.45	-7.45	114.16	-12.81	-7.26	-10.79	-13.13	-7.29	-11.62	98	54	87	54%	1.44	1.1	124.56
2018	117	115	4557	15.8	1.64	1.01	1.58	2.90	117.06	4.75	2.94	4.57	-4.03	-2.16	-3.11	-12	-6	-9		1.46	1.12	126.53
2019	116	114	4022	13.5	1.62	0.89	1.35	-1.26	115.80	-2.04	-1.13	-1.70	1.35	0.91	1.44	-2	-1	-2		1.35	1.03	116.46
2020	108	105	4418	12.9	1.50	0.98	1.29	-7.42	108.38	-11.09	-7.29	-9.56	-6.57	-4.21	-5.63	49	31	42	Y20-Y24	1.3	0.99	112.03
2021	104	94	4233	13.6	1.34	0.94	1.36	-4.54	103.84	-6.08	-4.27	-6.16	-8.58	-5.78	-7.86	39	26	36	293	1.25	0.95	107.86
2022	106	91	3819	10.8	1.30	0.85	1.08	2.12	105.96	2.77	1.80	2.29	-1.66	-1.24	-1.93	-4	-3	-4	46%	1.11	0.85	96.25
2023	110	89	3519	13.0	1.27	0.78	1.30	4.17	110.13	5.30	3.26	5.42	4.03	2.53	3.85	17	11	16		1.16	0.89	100.44
2024	103	92	4202	12.6	1.32	0.93	1.26	-7.00	103.13	-9.24	-6.54	-8.79	-1.97	-1.64	-1.69	14	11	12		1.2	0.92	103.99
Avg	113	106	4027	13.6	1.51	0.89	1.36	-2.66	112.98	-4.19	-2.58	-3.72	-3.73	-2.25	-3.28	254	153	227		1.31	1	114
Correl.	100%	85%	-46%	57%										SD-E:	634	40%	24%	36%			R =	83%

AI					/ 70	/ 4500	/10	S. Rate	Strain	Strs 1	Strs 2	Strs 3	Hgt 1	Hgt 2	Hgt 3	Area 1	Area 2	Area 3	Time	Pred.	Pred.	Pred.
2/6/24	PPG AI	FPG	Steps	Carbs AI	FPG	Steps	PPG AI	PPG AI	PPG AI	FPG	Steps	Carbs AI	FPG	Steps	Carbs AI	FPG	Steps	Carbs AI	Zone	Step 1	Step 2	PPG AI
2015	132	123	3036	14.9	1.76	0.67	1.49	0.00	132.10	0.00	0.00	0.00	0.00	0.00	0.00	0	0	0	Y15-Y19	1.41	1.05	132.1
2016	121	117	4084	14.8	1.67	0.91	1.48	-10.88	121.22	-18.12	-9.87	-16.11	-9.06	-4.94	-8.06	99	54	88	458	1.42	1.06	120.87
2017	115	120	4382	14.9	1.72	0.97	1.49	-6.44	114.78	-11.07	-6.27	-9.60	-14.60	-8.07	-12.86	94	52	83	62%	1.46	1.09	124.33
2018	116	115	4557	14.7	1.64	1.01	1.47	1.36	116.14	2.23	1.38	2.00	-4.42	-2.45	-3.80	-6	-3	-5		1.43	1.07	121.63
2019	117	114	4022	15.2	1.62	0.89	1.52	0.87	117.01	1.41	0.78	1.32	1.82	1.08	1.66	2	1	1		1.41	1.06	120.2
2020	110	105	4418	14.5	1.50	0.98	1.45	-7.21	109.80	-10.78	-7.08	-10.45	-4.68	-3.15	-4.56	34	23	33	Y20-Y24	1.36	1.02	115.6
2021	104	94	4233	13.9	1.34	0.94	1.39	-5.45	104.35	-7.29	-5.13	-7.59	-9.04	-6.10	-9.02	49	33	49	285	1.26	0.95	107.72
2022	107	91	3819	13.1	1.30	0.85	1.31	2.52	106.87	3.29	2.14	3.29	-2.00	-1.49	-2.15	-5	-4	-5	38%	1.2	0.9	102.03
2023	110	89	3519	13.1	1.27	0.78	1.31	3.24	110.11	4.12	2.53	4.24	3.70	2.34	3.77	12	8	12		1.17	0.88	99.57
2024	103	92	4202	12.9	1.32	0.93	1.29	-6.88	103.23	-9.08	-6.42	-8.90	-2.48	-1.95	-2.33	17	13	16		1.22	0.91	103.88
Avg	114	106	4027	14.2	1.51	0.89	1.42	-2.89	113.56	-4.53	-2.79	-4.18	-4.08	-2.47	-3.74	295	176	272		1.33	1	115
Correl.	100%	85%	-50%	72%										SD-E:	743	40%	24%	37%			R =	85%

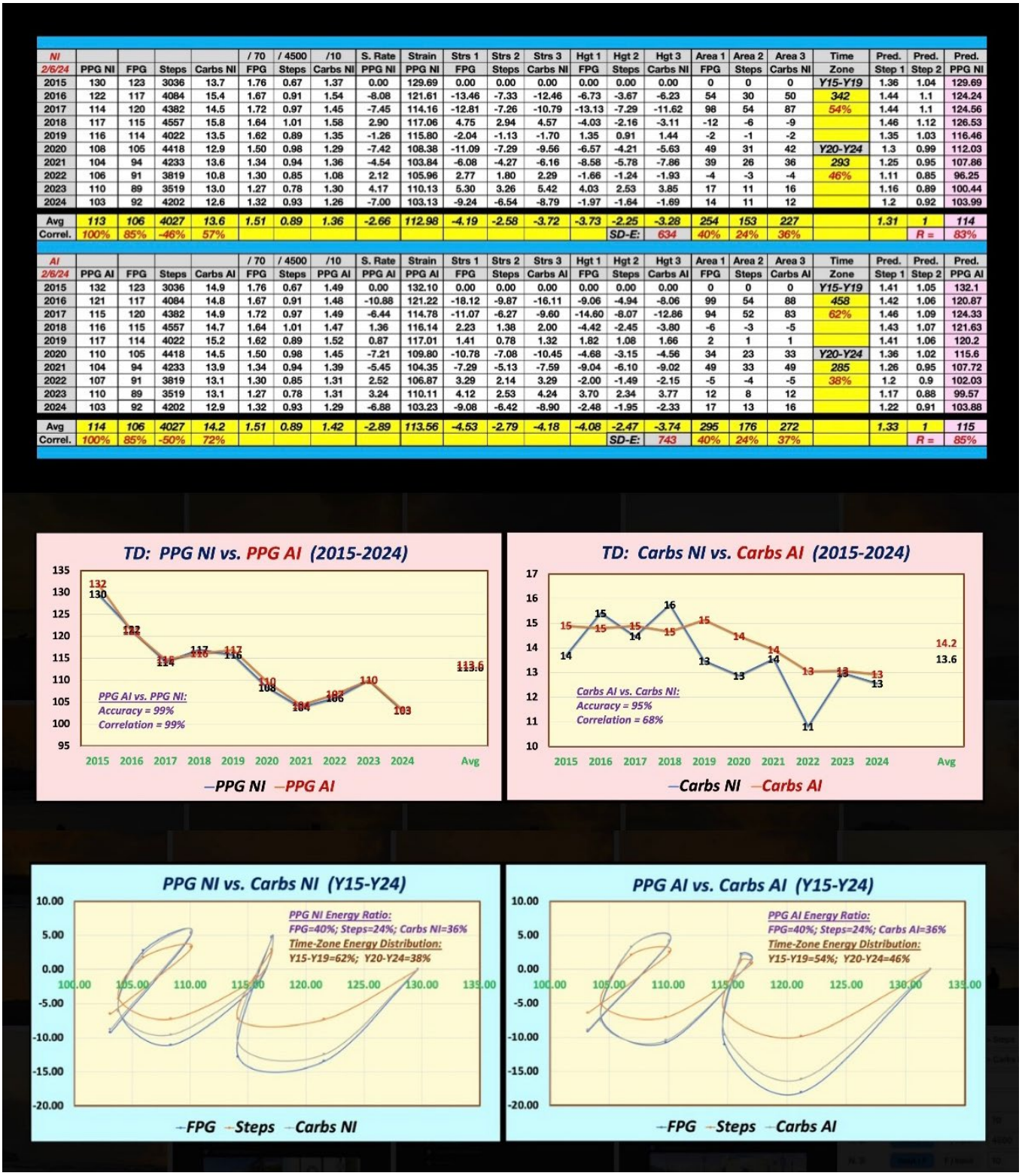

Figure 1. shows Data table, TD and SD results.

8. Conclusions

In summary, the findings reveal that the Carbs AI and Carbs NI models achieve 95% prediction accuracy and 68% correlation. Additionally, the PPG AI and PPG NI models attain 99% prediction accuracy and 99% of correlation.

The SD-VMT approach outlines energy distributions for PPG and Carbs, highlighting identical outcomes except in time-zone energy distributions.

Insulin (FPG): 40%,

Carbs (energy intake): 36%,

Steps (energy expenditure): 24%.

It is specifically noted that ***Carbs to Steps ratio is around 1.5***

which means diet is more important than exercise.
Time-zone energy distributions between AI and NI are different for Carbs and PPG, as follows:
For Carbs:
62% for Y15-Y19 vs. 38% for Y29-Y24.
For PPG:
54% for Y15-Y19 vs. 46% for Y29-Y24.

Key Message

The author demonstrates that AI technology, grounded in optical physics and wave theory, delivers high predictive accuracy and valuable insights into the interplay between beta cell insulin status, physical activity, and carbohydrate/sugar intake amount.

References

For editing purposes, majority of the references in this paper, which are self-references, have been removed for this article. Only references from other authors' published sources remain. The bibliography of the author's original self-references can be viewed at www.eclairemd.com.

For reading more of the author's published VGT or FD analysis results on medical applications, please locate them through platforms for scientific research publications, such as ResearchGate, Google Scholar, etc.